Rapid Communications

Pure spin current generation via photogalvanic effect with spatial inversion symmetry

Xixi Tao,[1,2,3] Peng Jiang,[1,3] Hua Hao,[1] Xiaohong Zheng,[1,2,3,*] Lei Zhang,[2,4,†] and Zhi Zeng[1,3]

[1]*Key Laboratory of Materials Physics, Institute of Solid State Physics, HFIPS, Chinese Academy of Sciences, Hefei 230031, China*

[2]*State Key Laboratory of Quantum Optics and Quantum Optics Devices, Institute of Laser Spectroscopy, Shanxi University, Taiyuan 030006, China*

[3]*Science Island Branch of Graduate School, University of Science and Technology of China, Hefei 230026, China*

[4]*Collaborative Innovation Center of Extreme Optics, Shanxi University, Taiyuan 030006, China*

(Received 31 March 2020; revised 15 July 2020; accepted 31 July 2020; published 18 August 2020)

We propose a new idea to generate pure spin current with photogalvanic effect (PGE) by designing devices with spatial inversion symmetry based on two-dimensional spin semiconducting materials. Due to the preservation of spatial inversion symmetry, the electric current generated by the PGE must be zero. However, finite spin-dependent current $I_{\uparrow/\downarrow}$ may still be produced. Once an amount of spin-up electrons flow into the device region from lead α and flow out from lead β under light irradiation, the same amount of spin-down electrons will flow into the device region from lead β and flow out from lead α, which results in $I_c^{\alpha/\beta} = I_\uparrow^{\alpha/\beta} + I_\downarrow^{\alpha/\beta} = 0$ and $I_s^{\alpha/\beta} = I_\uparrow^{\alpha/\beta} - I_\downarrow^{\alpha/\beta} \neq 0$ simultaneously for each lead and thus finite pure spin current arises. As a concrete example, this idea is demonstrated by calculating the PGE in a photoelectric device constructed with an armchair-edged graphene nanoribbon which is divided into two semi-infinite ribbons. The two semi-infinite ribbons are then periodically and symmetrically patterned with ferromagnetic triangle antidots in the form of "$\triangleright\triangleleft$" to achieve spatial inversion symmetry of the device. We find that the pure spin current can be robustly generated, neither dependent on the photon energy and polarization/helicity angle, nor dependent on whether it is linearly, circularly, or elliptically polarized.

DOI: 10.1103/PhysRevB.102.081402

Pure spin current is characterized by the current of spin accompanied by no net current of charge in a device [1]. Since spin and charge are both the intrinsic degrees of freedom of electrons and the flow of each electron carries charge current and spin current simultaneously, pure spin current can only be achieved when there are equal numbers of spin-up and spin-down electrons flowing in opposite directions. Since it is a low-dissipation process, together with no Joule heat arising from the charge current, spin current is of central importance in spintronics due to its low energy consumption and has received intensive attention. The generation and detection are two major tasks in the study of pure spin current. As for generation, it has been achieved in different materials by various ways, such as spin Hall effect induced by spin-orbit coupling [2], adiabatic quantum pumping [3,4], optical injection [5], spin-dependent Seebeck effect [6–8], voltage control in three-terminal devices [9], current injection from a ferromagnet to a semiconductor [10], etc.

As an alternative driving force apart from bias voltage for generating electrical current, light irradiation has received increasing attention in recent years [11,12]. It works by shedding light on the central region of a photoelectric device to excite electrons in the valence band to the conduction band and then these excited electrons flow to the two leads with unequal probability, which leads to a net current. Photocurrent can be generated in systems lacking spatial inversion symmetry, which is called the photogalvanic effect (PGE), first proposed independently by Ivchenko and Pikus [13] and Belinicher [14], and observed experimentally by Asnin *et al.* [15] in traditional semiconductors, followed by intensive exploration ever since [16–23]. In particular, the application of PGE in pure spin current generation has been widely studied in traditional semiconductors, where a linear-in-k term in the Hamiltonian arising from spin-orbit interaction due to spatial inversion asymmetry leads to the spin splitting along certain k direction and plays the key role in the pure spin current generation [24–28].

With the rise of two-dimensional (2D) materials and their promising application in nanoscale electronic devices in recent years, interests of PGE in photocurrent generation have also been initiated in 2D systems where the structures are designed to lose spatial inversion symmetry purposely [29,30] or a small bias across the devices is applied to induce asymmetry in the real space electronic structure [31–34]. Interestingly, the PGE-induced pure spin current has also been predicted in quite a few 2D magnetic or spin-polarized systems, such as zigzag SiC nanoribbons [35], triangulene [36], silicene nanoribbons [37], and Ni/phosphorene/Ni junction [38]. However, the conditions for obtaining pure spin current in these systems are prohibitively strict since it can be achieved only by precisely tuning the photons at specific energy or specific polarization/helicity angle, which is rather difficult practically. Thus, a much more robust scheme to

*xhzheng@theory.issp.ac.cn
†zhanglei@sxu.edu.cn

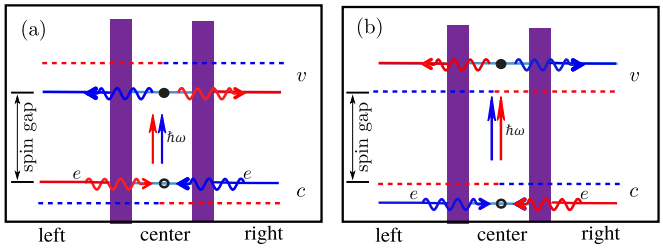

FIG. 1. Two kinds of processes of pure spin current generation occurring between two spin subbands with (a) the spin gap and (b) a larger gap. v and c indicate the valence and conduction bands while red and blue lines are for spin-up and spin-down channels, respectively.

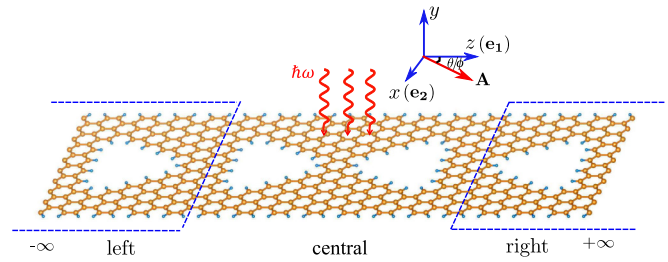

FIG. 2. The device structure where the two halves of the 19-AGNR are symmetrically patterned by triangle antidots with zigzag edges. The device is divided into three regions: left lead, central region, and right lead. Light is normally irradiated on the central region. $\mathbf{A}$ is the electromagnetic vector potential. $\mathbf{e}_1$ and $\mathbf{e}_2$ are two unit vectors for defining the polarization of the light, with the angle $\theta(\phi)$ between $\mathbf{e}_1$ and $\mathbf{A}$ defined as the polarization/helicity angle.

avoid these demanding conditions is highly desired. In this Rapid Communication, we will demonstrate that although systems with spatial inversion symmetry are not capable of generating charge current based on PGE, they may serve as perfect candidates for generating pure spin current, in the sense that the generation is neither dependent on the photon energy and polarization/helicity angle, nor dependent on whether it is linearly polarized, circularly polarized, or elliptically polarized.

It is well known that PGE is purely a nonlinear optical response of materials to light [13,14] and the PGE-induced current arises from the quadratic term of the alternating electric field E which gives rise to a *direct* charge current density, $j = \alpha EE^*$, where α is the PGE coefficient. Because reversing the direction of E will reverse the flow of charge current, from j to $-j$, j must vanish if $\alpha(\mathbf{r}) = \alpha(-\mathbf{r})$. j will be finite only when the material has no spatial inversion symmetry which definitely holds $\alpha(\mathbf{r}) \neq \alpha(-\mathbf{r})$. Thus far, basically all of the PGE studies have been performed under the condition of $\alpha(\mathbf{r}) \neq \alpha(-\mathbf{r})$, including the generation of pure spin current with PGE [35–38]. For pure spin current, of course we need $\alpha(\mathbf{r}) = \alpha(-\mathbf{r})$, so that the total charge current is zero. However, $\alpha(\mathbf{r})$ is spin resolved for spin-polarized systems, which means $\alpha(\mathbf{r}) = \alpha_\uparrow(\mathbf{r}) + \alpha_\downarrow(\mathbf{r})$. There are two ways to satisfy $\alpha(\mathbf{r}) = \alpha(-\mathbf{r})$: (1) $\alpha_\uparrow(\mathbf{r}) = \alpha_\uparrow(-\mathbf{r})$ and $\alpha_\downarrow(\mathbf{r}) = \alpha_\downarrow(-\mathbf{r})$; and (2) $\alpha_\uparrow(\mathbf{r}) = \alpha_\downarrow(-\mathbf{r})$ and $\alpha_\downarrow(\mathbf{r}) = \alpha_\uparrow(-\mathbf{r})$. For (1), we will have both $j_\uparrow = 0$ and $j_\downarrow = 0$, which is trivial. However, for (2), we will have $j_\uparrow \neq 0$ and $j_\downarrow \neq 0$ but $j_\uparrow + j_\downarrow = 0$, which is nontrivial and corresponds to pure spin current. Therefore, what we need is to find or design systems that have $\alpha_\uparrow(\mathbf{r}) = \alpha_\downarrow(-\mathbf{r})$ and $\alpha_\downarrow(\mathbf{r}) = \alpha_\uparrow(-\mathbf{r})$. In density functional theory, all physical properties of a system are solely determined by its charge density, thus we must have the spin-dependent charge density $\rho_\uparrow(\mathbf{r}) = \rho_\downarrow(-\mathbf{r})$ and $\rho_\downarrow(\mathbf{r}) = \rho_\uparrow(-\mathbf{r})$. This naturally gives rise to the spin density $\Delta\rho(\mathbf{r}) = -\Delta\rho(-\mathbf{r})$, which means antisymmetrical distribution of the spin density and antiferromagnetic coupling between any two atoms with respect to the inversion center.

Figure 1 shows our design principle based on spin semiconducting 2D materials. The whole device consists of two semi-infinite parts, and each part is a spin semiconductor characterized by the top valence subband from one spin channel and the bottom conduction subband from the other spin channel [39]. The band structures of the left and right parts will overlap with each other after simply exchanging the spin indices. As shown in Figure. 1(a), under light irradiation with photon energy slightly larger than the spin gap, the spin-up electrons excited from the left lead can only move to the right due to spin matching while the same amount of spin-down electrons excited from the right lead can only move to the left, resulting in right-flowing pure spin current. With a larger photon energy, the excitation may occur between two subbands with a larger gap, resulting in a left-flowing pure spin current, as shown in Fig. 1(b). Thus, the central task is to search or design structures that will have opposite band structures and antisymmetrical spin density for the two leads in their ground state. We will show that graphene with two sublattices ("A" and "B") with some structure design is an ideal material to realize this, and specifically, armchair-edged graphene nanoribbons (AGNRs) periodically patterned by triangle antidots with zigzag edges will exchange the two spin indices by reversing the directions of the triangles. Graphene antidots are nanopores formed by cutting graphene molecules away from the graphene. Antidot as a tuning strategy of properties of graphene and other 2D materials has been widely investigated both theoretically and experimentally [40–47], and antidot arrays with various shapes in graphene have been fabricated experimentally [46,47].

In the following, an AGNR with a width of 19 dimer lines (abbreviated as 19-AGNR) periodically patterned with triangle zigzag-edged antidots will be taken as an example. The size of the antidot defined as the number n of edge C atoms of each zigzag edge is chosen as $n = 4$. The photoelectric device constructed with the AGNR is divided into two halves, with the triangle antidots in the left half directed towards the right ("$\triangleright$") while those in the right half are directed towards the left ("$\triangleleft$"). Thus, the two triangles in the central region have a face-to-face configuration (namely, "$\triangleright\triangleleft$"). The left lead supercell, the central region, and the right lead supercell of the device, with lengths of 17.04, 34.08, and 17.04 Å, including four, eight, and four primitive armchair unit cells, respectively, are shown in Fig. 2. The dangling bonds of the edge C atoms are passivated by H atoms to avoid edge reconstruction [48,49]. Linearly or elliptically polarized light is vertically irradiated at the central region. The photon is described by its energy $\hbar\omega$ and polarization (helicity) angle $\theta(\phi)$. Structure

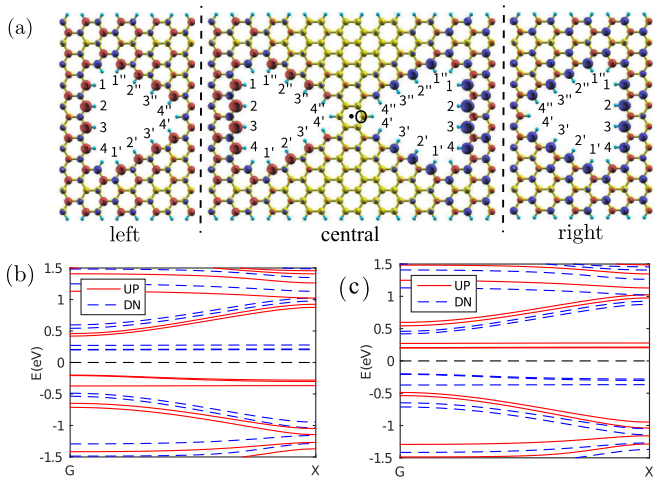

FIG. 3. (a) The spin density of the left lead, central region, and right lead, with O the spatial inversion center and the numbers indicating the edge carbon sites; and the band structure of (b) the left lead and (c) the right lead.

relaxation is performed by density functional theory (DFT) calculations with the SIESTA code [50], while self-consistent two-probe calculations and subsequent photocurrent calculations are performed by NANODCAL [51], a package combining DFT and nonequilibrium Green's functions for quantum transport study. The calculation details and formalism of photocurrent calculation is found in the Supplemental Material (SM) [52], which includes Refs. [53–60].

We first study the electronic structure of antidots periodically introduced in the 19-AGNR. It is now well known that localized edge states and edge magnetism will be formed at any zigzag edges of graphene [61] and the edge magnetism has been successfully detected experimentally [62]. In graphene, the atomic magnetic moments on any two nearest neighbors are always antiferromagnetic (AFM), which means that the atomic magnetic moments on the two sublattices will have opposite signs. This is determined by the spin alteration rule stating that for the stabilization of unpaired electrons, the different sublattices have AFM spin coupling [63,64]. The supercell structure and spin density are shown in the left panel in Fig. 3(a). The edge magnetic moments of the antidot are shown in Table S1 in the SM [52]. It is seen that all the edge magnetic moments have the same sign, similar to those of the graphene molecule with the same shape and size [see Fig. S1(a) and Table S1 in the SM [52]], indicating that the coupling among all three edges of the antidot is ferromagnetic. This is easy to understand since all the edge C atoms of the antidot are located at the same sublattice (say, "A"). The calculated total magnetic moment is $3.0\mu_B$, in good agreement with the predictions of Lieb's theorem [65] which states that the total spin S of the exact ground state of the Hubbard model in bipartite lattices satisfies $2S = N_A - N_B$, with N_A and N_B the number of atoms in the sublattices A and B. More importantly, the 19-AGNR now becomes a spin semiconductor, with a spin gap of 0.4 eV between the two nearest subbands around the Fermi level, as seen from the band structure shown in Fig. 3(b).

Further, such an antidot patterned graphene nanoribbon is used to construct a photoelectric device, with the antidots in the left half directed towards the right ("$\triangleright$") and those in the right half directed towards the left ("$\triangleleft$"), as shown in Fig. 2. Analysis indicates that the edge C atoms in the two antidots with reversed directions in the central region are located on the different sublattices. Thus, the edge magnetic moments in these two antidots are opposite, resulting in antiferromagnetic coupling between them due to the spin alteration rule [see the middle panel of Fig. 3(a)]. Actually, the total energy calculation of the central region under the exchange-correlation functional with generalized gradient approximation in the form of Perdew, Burke, and Ernzerhof suggests that the AFM coupling state between the two antidots is the ground state, with 58.7 meV lower than the ferromagnetic (FM) coupling state [52]. More accurate calculations to consider the electron-electron interaction with the HSE06 hybrid functional gives the AFM-FM total energy difference of 322.6 meV [52], suggesting that the AFM ground state is very stable. Naturally, compared with the left lead, the magnetic moment in the right lead is reversed [see Table S1 and the right panel of Fig. 3(a)] and the two spin channels in the band structure are exchanged with each other [compare Figs. 3(b) and 3(c)]. The spin density in Fig. 3(a) shows clearly the ground state magnetic configurations of the system, namely, AFM coupling between the antidots of the left and right leads. Note that we will neglect the situation of FM coupled antidots in the central region because AFM coupling is the ground state. In addition, when there is light excitation, due to the spin selection rule dictated by quantum mechanics, it is physically impossible to change the AFM coupling to FM coupling under optical excitation considered in this work (for detailed reasons, see the SM [52]).

Next, we study the photocurrent induced by PGE in this system. First, the spin-dependent photocurrents as a function of photon energy under linearly polarized light with polarization angle $\theta = 0$ are shown in Fig. 4(a). Very interestingly, both the spin-up and spin-down components are finite in a large energy range, although the system has spatial inversion symmetry in structure. This is because for each spin component, the charge density is not invariant under spatial inversion. More interestingly, the photocurrents of the two spin channels always have the same magnitude but opposite signs, which means the net charge current will always be zero according to $I_c = I_\uparrow + I_\downarrow$ while the spin current $I_s = I_\uparrow - I_\downarrow$ is not. Thus, pure spin current is generated. Further investigation indicates that the pure spin current generated is so robust that its occurrence is sensitive neither to the polarization angle, nor to whether the light is linearly or elliptically polarized. Figures 4(b) and 4(c) show the spin-dependent photocurrents as a function of polarization or helicity angle under a linearly or elliptically polarized light with $\hbar\omega = 1.00$ eV. Both the spin channels satisfy $I_{\uparrow/\downarrow} = \pm a\cos(2\theta)$ or $\pm a\cos(2\varphi)$, indicating that both spin channels always have equal finite photocurrent with opposite signs.

The robustness of the pure spin current generation independent of polarization/helicity angle is governed by the spin semiconducting feature and spatial inversion symmetry of the device. In devices with spatial inversion symmetry, we can guarantee both the opposite signs and equal magnitudes of

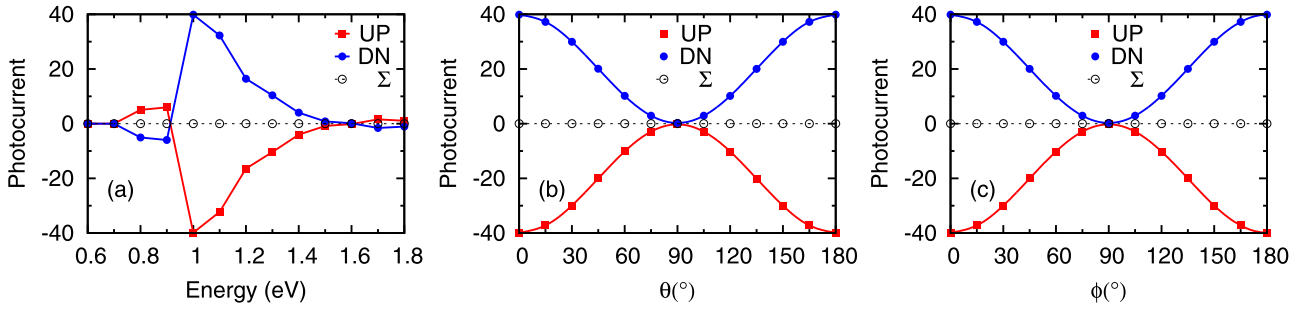

FIG. 4. The photocurrent as a function of (a) photon energy under linearly polarized light with polarization angle $\theta = 0^\circ$; (b) polarization angle θ under linearly polarized light with photon energy $E = 1.0$ eV; (c) helicity angle ϕ under elliptically polarized light with $E = 1.0$ eV. $\phi = 45^\circ$ and 135° mean right and left circularly polarized light, respectively. "UP," "DN," and "Σ" mean the contributions of the spin-up channel, spin-down channel, and their sum.

the two spin channels at any photon energy and polarization angle because the charge densities of the two spin channels are antisymmetric with respect to the inversion center along any direction. During the process, the situation that electrons of one spin channel experience along one direction will be exactly the same as the one experienced by the electrons of the other spin channel along the opposite direction. Thus, when the photon energy is increased to be larger than the spin gap, for example, 0.8 eV, under the light irradiation, once an amount of spin-up electrons with certain energy from a valence band of the left lead flows into the central region, they will always flow out from the right lead due to spin matching in the conduction band, as clarified in Fig. 1(a). Meanwhile, the same amount of spin-down electrons with the same energy will flow in from the right lead and then flow out from the left lead due to the spin semiconducting feature and spatial inversion symmetry of the device. This gives rise to zero charge current $I_c^\alpha = I_\uparrow^{\text{in}} + I_\downarrow^{\text{out}} = 0$ and finite spin current $I_s^\alpha = I_\uparrow^{\text{in}} - I_\downarrow^{\text{out}} = 2I_\uparrow^{\text{in}}$. In addition, we can understand, with the increase of the photon energy, why both the spin channels reverse their signs by the generation process shown in Fig. 1(b), which leads to the change of the pure spin current direction. With the increase of the photon energy, the electron excitation will occur between two subbands with a larger gap. In this situation, the electrons of spin-down channel in the left lead and those of the spin-up channel in the right lead with lower energy in the valence band will participate in the current generation process, leading to left-flowing spin-up current and equal right-flowing spin-down current. Actually, the reverse of spin indices of the two leads of the same kind of materials as shown in Fig. 1 may be simply achieved by applying opposite magnetic fields to them; however, pure spin current independent of polarization or helicity angle cannot be obtained if the system lacks spatial inversion symmetry, just as reported in previous works where pure spin current is achieved in systems with C_s symmetry by reversing the magnetization of the two leads with magnetic field, but obtained only at the special polarization/helicity angles of 0°, 90°, and 180° [37,38]. The mechanism of PGE-induced pure spin current presented in this work is totally different from that observed in traditional semiconductors [24–28] and previously reported 2D semiconductors [37,38] where spatial inversion asymmetry must be imposed. In broken spatial inversion symmetry systems, one must judiciously adjust device parameters to find points of operation with zero charge current. In comparison, in systems with spatial inversion symmetry, PGE can generate pure spin current regardless of the photon energy, polarization type, and polarization angle, and such pure spin current flows out of the system without, automatically, any accompanying charge current.

Finally, we show that the scheme can be made much simpler by introduction of an antidot pair of the shape "▷ ◁" or a single rectangular antidot with two antiferromagnetically coupled zigzag edges only in the central region but not in the leads. Calculations show that pure spin current can always be produced, independent of the photon energy, polarization angle, and polarization type. This arises from the antisymmetric spin density due to the spatial inversion symmetry of the structure (see the SM [52]). These extra examples greatly decrease the complexity of the structure design and the difficulty of functionalization of the graphene nanoribbons.

In conclusion, we propose that the photogalvanic effect under spatial inversion symmetry is a promising route to generate pure spin current with two-dimensional spin semiconducting materials among which AGNRs containing triangle antidots with zigzag edges are a good example. The strategy is quite robust in the sense that, unlike any other already reported systems in which pure spin current can only be achieved at specific photon energy and specific polarization angle, the pure spin current obtained with our strategy is neither dependent on the photon energy or polarization energy, nor dependent on whether it is linearly polarized or elliptically polarized. Thus, it is not necessary to precisely tune the photon energy or polarization angle as done in previous works. The idea can be readily extended to other 2D spin semiconductors, and more generally, to any nonmagnetic systems with spatial inversion symmetry functionalized with two antiferromagnetic coupled ferromagnets which can be magnetic molecules, clusters, defects, or quantum dots.

We gratefully acknowledge financial support by the National Natural Science Foundation of China under Grants No. 11974355 and No. 11704232; National Key R&D Program of China under Grant No. 2017YFA0304203; the Program of State Key Laboratory of Quantum Optics and Quantum Optics Devices (Grant No. KF201810); and Shanxi Province

100-Plan Talent Program and 1331KSC. Calculations were performed in Center for Computational Science of CASHIPS, the ScGrid of Supercomputing Center, and Computer Network Information Center of Chinese Academy of Sciences.

[1] Q. F. Sun and X. C. Xie, Phys. Rev. B **72**, 245305 (2005).
[2] J. E. Hirsch, Phys. Rev. Lett. **83**, 1834 (1999).
[3] E. R. Mucciolo, C. Chamon, and C. M. Marcus, Phys. Rev. Lett. **89**, 146802 (2002).
[4] Q.-F. Sun, H. Guo, and J. Wang, Phys. Rev. Lett. **90**, 258301 (2003).
[5] J. Hübner, W. W. Rühle, M. Klude, D. Hommel, R. D. R. Bhat, J. E. Sipe, and H. M. van Driel, Phys. Rev. Lett. **90**, 216601 (2003).
[6] P. Jiang, X. X. Tao, H. Hao, L. L. Song, X. H. Zheng, L. Zhang, and Z. Zeng, 2D Mater. **4**, 035001 (2017).
[7] P. Jiang, X. X. Tao, L. L. Kang, H. Hao, L. L. Song, J. Lan, X. H. Zheng, L. Zhang, and Z. Zeng, J. Phys. D: Appl. Phys. **52**, 015303 (2018).
[8] Y. H. Zhou and X. H. Zheng, J. Phys.: Condens. Matter **31**, 315301 (2019).
[9] Z. Ma, R. L. Wu, Y. B. Yu, and M. Wang, J. Appl. Phys. **116**, 043706 (2014).
[10] S. O. Valenzuela and M. Tinkham, Nature (London) **442**, 176 (2006).
[11] Y. Luo, Y. Xie, X. Ye, and Y. Wang, Phys. Chem. Chem. Phys. **21**, 7613 (2019).
[12] Y. Luo, Y. Hu, and Y. Xie, J. Mater. Chem. A **7**, 27503 (2019).
[13] E. L. Ivchenko and G. E. Pikus, JETP Lett. **27**, 604 (1978).
[14] V. I. Belinicher, Phys. Lett. A **66**, 213 (1978).
[15] V. M. Asnin, A. A. Bakun, A. M. Danishevskii, E. L. Ivchenko, G. E. Pikus, and A. A. Rogachev, JETP Lett. **28**, 74 (1978).
[16] P. Král, E. J. Mele, and D. Tománek, Phys. Rev. Lett. **85**, 1512 (2000).
[17] X. W. He, B. Shen, Y. H. Chen, Q. Zhang, K. Han, C. M. Yin, N. Tang, F. J. Xu, C. G. Tang, Z. J. Yang, Z. X. Qin, G. Y. Zhang, and Z. G. Wang, Phys. Rev. Lett. **101**, 147402 (2008).
[18] A. G. Mal'shukov, Phys. Rev. Lett. **107**, 146603 (2011).
[19] Y. Gao, Y. Zhang, and D. Xiao, Phys. Rev. Lett. **124**, 077401 (2020).
[20] S. Dhara1, E. J. Mele, and R. Agarwal, Science **349**, 726 (2015).
[21] S.-Y. Xu, Q. Ma, H. Shen, V. Fatemi, S. Wu, T.-R. Chang, G. Chang, A. M. M. Valdivi, C.-K. Chan, Q. D. Gibson, J. Zhou, Z. Liu, K. Watanabe, T. Taniguchi, H. Lin, R. J. Cava, L. Fu, N. Gedik, and P. Jarillo-Herrero, Nat. Phys. **14**, 900 (2018).
[22] H. Yuan, X. Wang, B. Lian, H. Zhang, X. Fang, B. Shen, G. Xu, Y. Xu, S. C. Zhang, and H. Y. Hwang, Nat. Nanotechnol. **9**, 851 (2014).
[23] Z. Ji, G. Liu, Z. Addison, W. Liu, P. Yu, H. Gao, Z. Liu, A. M. Rappe, C. L. Kane, E. J. Mele, and R. Agarwal, Nat. Mater. **18**, 955 (2019).
[24] E. L. Ivchenko and S. A. Tarasenko, Semicond. Sci. Technol. **23**, 114007 (2008).
[25] B. Zhou and S.-Q. Shen, Phys. Rev. B **75**, 045339 (2007).
[26] S. Ganichev, V. Bel'kov, S. Tarasenko, S. Danilov, S. Giglberger, C. Hoffmann, E. Ivchenko, D. Weiss, W. Wegscheider, C. Gerl, and D. Schuh, Nat. Phys. **2**, 609 (2006).
[27] S. A. Tarasenko and E. L. Ivchenko, JETP Lett. **81**, 231 (2005).
[28] E. L. Ivchenko and S. D. Ganichev, arXiv:1710.09223.
[29] J. Chen, Y. Hu, and H. Guo, Phys. Rev. B **85**, 155441 (2012).
[30] Y. Xie, L. Zhang, Y. Zhu, L. Liu, and H. Guo, Nanotechnology **26**, 455202 (2015).
[31] L. Zhang, K. Gong, J. Chen, L. Liu, Y. Zhu, D. Xiao, and H. Guo, Phys. Rev. B **90**, 195428 (2014).
[32] X. Tao, L. Zhang, X. Zheng, H. Hao, X. Wang, L. Song, Z. Zeng, and H. Guo, Nanoscale **10**, 174 (2018).
[33] P. Zhao, J. Li, W. Wei, Q. Sun, H. Jin, B. Huang, and Y. Dai, Phys. Chem. Chem. Phys. **19**, 27233 (2017).
[34] F. Chu, M. Chen, Y. Wang, Y. Xie, B. Liu, Y. Yang, X. An, and Y. Zhang, J. Mater. Chem. C **6**, 2509 (2018).
[35] J. Chen, L. Zhang, L. Zhang, X. Zheng, L. Xiao, S. Jia, and J. Wang, Phys. Chem. Chem. Phys. **20**, 26744 (2018).
[36] H. Jin, J. Li, T. Wang, and Y. Yu, Carbon **137**, 1 (2018).
[37] P. Jiang, L. Kang, X. Tao, N. Cao, H. Hao, X. Zheng, L. Zhang, and Z. Zeng, J. Phys.: Condens. Matter **31**, 495701 (2019).
[38] Y. Xie, M. Chen, Z. Wu, Y. Hu, Y. Wang, J. Wang, and H. Guo, Phys. Rev. Appl. **10**, 034005 (2018).
[39] Z. F. Wang, S. Jin, and F. Liu, Phys. Rev. Lett. **111**, 096803 (2013).
[40] T. G. Pedersen, C. Flindt, J. Pedersen, N. A. Mortensen, A.-P. Jauho, and K. Pedersen, Phys. Rev. Lett. **100**, 136804 (2008).
[41] T. Shen, Y. Q. Wu, M. A. Capano, L. R. Rokhinson, L. W. Engel, and P. D. Ye, Appl. Phys. Lett. **93**, 122102 (2008).
[42] F. Ouyang, S. Peng, Z. Liu, and Z. Liu, ACS Nano **5**, 4023 (2011).
[43] T. Gunst, T. Markussen, A.-P. Jauho, and M. Brandbyge, Phys. Rev. B **84**, 155449 (2011).
[44] X. H. Zheng, G. R. Zhang, Z. Zeng, V. M. García-Suárez, and C. J. Lambert, Phys. Rev. B **80**, 075413 (2009).
[45] G. Calogero, I. Alcón, N. Papior, A.-P. Jauho, and M. Brandbyge, J. Am. Chem. Soc. **141**, 13081 (2019).
[46] C. Moreno, M. Vilas-Varela, B. Kretz, A. Garcia-Lekue, M. V. Costache, M. Paradinas, M. Panighel, G. Ceballos, S. O. Valenzuela, D. Pena, and A. Mugarza, Science **360**, 199 (2018).
[47] M. Shekhirev, P. Zahl, and A. P. Sinitskii, ACS Nano **12**, 8662 (2018).
[48] L. L. Song, X. H. Zheng, R. L. Wang, and Z. Zeng, J. Phys. Chem. C **114**, 12145 (2010).
[49] X. Zhang, O. V. Yazyev, J. Feng, L. Xie, C. Tao, Y. C. Chen, L. Jiao, Z. Pedramrazi, A. Zettl, and S. G. Louie, ACS Nano **7**, 198 (2013).
[50] J. Soler, E. Artacho, J. D. Gale, A. Garcia, J. Junquera, P. Ordejon, and D. Sanchez-Portal, J. Phys.: Condens. Matter **14**, 2745 (2002).
[51] J. Taylor, H. Guo, and J. Wang, Phys. Rev. B **63**, 245407 (2001).
[52] See Supplemental Material at http://link.aps.org/supplemental/10.1103/PhysRevB.102.081402 for computational details and other results.
[53] J. P. Perdew, K. Burke, and M. Ernzerhof, Phy. Rev. Lett. **77**, 3865 (1996).
[54] G. Kresse and J. Furthmüller, Phys. Rev. B **54**, 11169 (1996).
[55] G. Kresse and D. Joubert, Phys. Rev. B **59**, 1758 (1999).
[56] P. E. Blöchl, Phys. Rev. B **50**, 17953 (1994).

[57] C. Cohen-Tannoudji, B. Diu, and F. Laloe, *Quantum Mechanics* (Wiley, New York, 1991), Vol. 2, pp. 1304–1315.
[58] L. E. Henrickson, J. Appl. Phys. **91**, 6273 (2002).
[59] F. Guinea, New J. Phys. **12**, 083063 (2010).
[60] H. Min, J. E. Hill, N. A. Sinitsyn, B. R. Sahu, L. Kleinman, and A. H. MacDonald, Phys. Rev. B **74**, 165310 (2006).
[61] Y.-W. Son, M. L. Cohen, and S. G. Louie, Nature (London) **444**, 347 (2006).
[62] M. Slota, A. Keerthi, W. K. Myers, E. Tretyakov, M. Baumgarten, A. Ardavan, H. Sadeghi, C. J. Lambert, A. Narita, K. Müllen, and L. Bogani, Nature (London) **557**, 691 (2018).
[63] J. A. Chan, B. Montanari, J. D. Gale, S. M. Bennington, J. W. Taylor, and N. M. Harrison, Phys. Rev. B **70**, 041403(R) (2004).
[64] L. Brey, H. A. Fertig, and S. Das Sarma, Phys. Rev. Lett. **99**, 116802 (2007).
[65] E. H. Lieb, Phys. Rev. Lett. **62**, 1201 (1989).